Wood Sci Technol (2015) 49:403–420
DOI 10.1007/s00226-015-0700-5

ORIGINAL

Composition and structure of balsa (*Ochroma pyramidale*) wood

Marc Borrega · Patrik Ahvenainen · Ritva Serimaa · Lorna Gibson

Received: 7 April 2014 / Published online: 23 January 2015

Abstract Balsa, with its low density and relatively high mechanical properties, is frequently used as the core in structural sandwich panels, in applications ranging from wind turbine blades to racing yachts. Here, both the cellular and cell wall structure of balsa are described, to enable multi-scale modeling and an improved understanding of its mechanical properties. The cellular structure consists of fibers (66–76 %), rays (20–25 %) and vessels (3–9 %). The density of balsa ranges from roughly 60 to 380 kg/m^3; the large density variation derives largely from the fibers, which decrease in edge length and increase in wall thickness as the density increases. The increase in cell wall thickness is predominantly due to a thicker secondary S2 layer. Cellulose microfibrils in the S2 layer are highly aligned with the fiber axis, with a mean microfibril angle (MFA) of about 1.4°. The cellulose crystallites are about 3 nm in width and 20–30 nm in length. The degree of cellulose crystallinity appears to be between 80 and 90 %, considerably higher than previously reported for other woods. The outstanding mechanical properties of balsa wood in relation to its weight are likely explained by the low MFA and the high cellulose crystallinity.

M. Borrega · L. Gibson (✉)
Department of Materials Science and Engineering, Massachusetts Institute of Technology, 77 Massachusetts Avenue, Cambridge, MA 02139, USA
e-mail: ljgibson@mit.edu

Present Address:
M. Borrega
Department of Forest Products Technology, Aalto University, PO Box 16300, 00076 Aalto, Finland

P. Ahvenainen · R. Serimaa
Department of Physics, University of Helsinki, PO Box 64, 00014 Helsinki, Finland

Introduction

Balsa (*Ochroma pyramidale*) is a tropical hardwood native to the Americas; its range extends from southern Mexico to Peru. Balsa seldom grows in dense stands, but rather as single trees that spring up in clearings in the rainforests, mixed with other tree species (Fletcher 1951). The scattering of balsa trees over large forested areas makes their harvesting difficult and expensive. For this reason, most balsa wood used commercially is harvested from plantations, particularly from Ecuador. Balsa is one of the fastest growing wood species, reaching about 20 m in height and up to 75 cm in diameter in 5–8 years (Fletcher 1951). Because of its fast growth, the wood density is very low, making balsa the lightest commercial timber available. Density values for balsa typically range between 100 and 250 kg/m^3, although they can vary as much as from 60 to 380 kg/m^3. The low density is extremely valuable in applications that require lightweight materials with good mechanical performance. Balsa wood is one of the preferred core materials in structural sandwich panels for wind turbine blades, sporting equipment, boats and aircraft.

The xylem (wood) in balsa, and hardwoods in general, is mainly composed of three types of cells: vessels, rays and fibers (Fig. 1). The volume fraction of fibers and rays in balsa has been reported to be about 80–90 and 8–15 %, respectively, with vessels making up the rest (Easterling et al. 1982; Da Silva and Kyriakides 2007). The fibers are long prismatic cells with relatively thick walls that provide mechanical support to the tree. The thickness of the double cell wall in balsa wood fibers ranges from 1 to 2.5 μm, increasing with density (Easterling et al. 1982; Da Silva and Kyriakides 2007). The wood cell wall consists of a primary layer and three secondary layers, the S1, S2 and S3. The S2 is the thickest layer, making up about 80–90 % of the total cell wall thickness in spruce tracheids (Fengel and Stoll 1973). In the secondary S1 and S3 layers, the cellulose microfibrils are oriented almost at 90° from the longitudinal cell axis, while in the

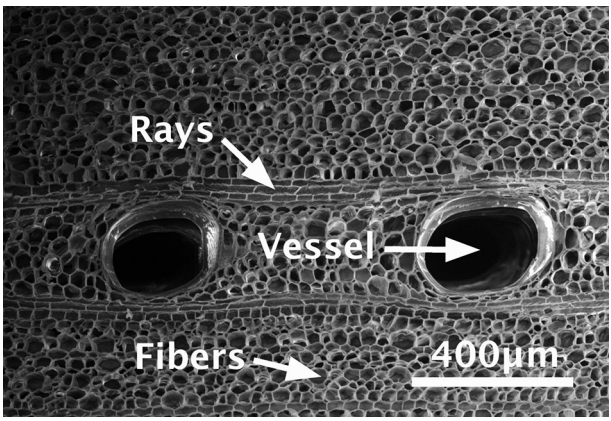

Fig. 1 SEM micrograph of the cross section of medium-density balsa showing the main type of cells

S2 layer they are mostly aligned with the longitudinal axis, with angles typically varying between 10° and 30° (Barnett and Bonham 2004; Donaldson 2008). Because of the thickness and the low microfibril angle (MFA), the S2 layer largely governs the axial mechanical properties of wood, particularly the stiffness (Cave 1968). The mechanical contribution of the S1 and S3 layers appears to be significant when wood is loaded in the transverse direction (Bergander and Salmén 2002).

Cellulose microfibrils contain both crystalline and amorphous regions, with the degree of crystallinity in the order of 40–60 % for both softwoods and hardwoods (Andersson et al. 2004; Wikberg and Maunu 2004; Penttilä et al. 2013). In the crystals, the cellulose chains are tightly bound, forming a highly ordered structure. However, disorder in cellulose chain packing tends to increase from the center toward the surfaces of the crystals (Ding and Himmel 2006; Fernandes et al. 2011). The cellulose crystallites in wood have been reported to be about 3–4 nm in width and about 20–30 nm in length (Hori et al. 2002; Peura et al. 2008; Penttilä et al. 2013). The crystalline structure of cellulose dominates the axial mechanical properties of wood, while the ligno-hemicellulosic matrix appears to have a more pronounced effect on the transverse mechanical properties (Bergander and Salmén 2002). In general, hardwoods contain about 40–45 % cellulose, 25–30 % hemicelluloses and 20–25 % lignin. Small amounts of organic (extractives) and inorganic (ash) compounds, typically below 5 %, can also be found outside the cell wall. In tropical woods such as balsa, the amount of extractives and ash may be considerably higher (Fengel and Wegener 2003).

The mechanical properties of balsa wood have been investigated, predominantly in compression, by Solden and McLeish (1976), Easterling et al. (1982), Vural and Ravichandran (2003) and Da Silva and Kyriakides (2007). The axial compressive Young's modulus and strength vary linearly with density, reaching values up to 6 GPa for modulus and 40 MPa for strength at the highest densities. Failure in compression tends to occur in the axial–tangential plane with the failure mode transitioning from plastic buckling of fibers to kink band formation as the density increases. Kink band formation in high-density balsa is facilitated by local misalignment of fibers due to the presence of rays, which leads to the development of shear stresses during compression. In the transverse direction, compressive modulus and strength vary to the cube and square of density, respectively, due to bending of the fiber cell walls. Transverse compressive modulus and strength values are about an order of magnitude lower than those in the axial direction. The rays act as reinforcement when balsa is loaded in the radial direction, with this effect being more pronounced in low-density balsa.

Since the mechanical behavior of wood depends on the cellular and cell wall structure, more detailed structural characterization of balsa is needed for multi-scale modeling and improved understanding of its mechanical properties, relevant to its use as a core material in sandwich panels as well as for the design of engineered materials inspired by balsa. In this paper, the cellular structure, the ultrastructure and the chemical composition of a wide range of densities of balsa wood are characterized and described.

Materials and methods

Balsa wood

End-grain balsa sheets with dimensions 76 mm in thickness, 610 mm in width and 1,219 mm in length were obtained from Baltek® (Baltek Inc., High Point, NC). The sheets, with commercial designations SB50, SB100 and SB150, had an apparent nominal density of 94, 153 and 247 kg/m^3, respectively. Each sheet was composed of small blocks of balsa (up to 100 × 100 mm^2) glued together, with each block originating from different parts of the tree as well as from different trees. The density of individual blocks varied at least sixfold, from about 60 to 380 kg/m^3. Balsa wood samples with densities below 100 kg/m^3, between 100 and 200 kg/m^3, and above 200 kg/m^3 are denoted as low-density (LD), medium-density (MD) and high-density (HD) balsa, respectively. The equilibrium moisture content of the balsa wood at room ambient conditions, determined by oven-drying representative samples at 103 °C for 24 h, was between 5 and 7 %.

Electron microscopy

The cell dimensions, the solid fraction and the volume fraction of each type of cell were measured using scanning electron microscopy. Balsa wood sections were cut by hand, using an industrial razor blade, from LD, MD and HD balsa cubes. A new blade was used for each cut. The MD and HD balsa cubes were boiled in water for about 15 min to soften them and thus facilitate their sectioning. All wood sections were air-dried and observed without coating in a JEOL JSM-6610LV scanning electron microscope (SEM). Micrographs were taken using the secondary electron detector in the SEM, operated at an accelerating voltage of 10–20 kV and in low-vacuum (30 Pa) mode. Changes in the working distance of the microscope resulted in errors in length measurement of about 2 %. Cell dimensions, volume fractions and solid fractions were determined from the micrographs using the open-source image processing software ImageJ 1.45 s.

The dimensions of the cell lumens in cross section were calculated by matching the cross-sectional area of individual cells to the area of an ellipse, a rectangle or a regular hexagon for vessels, rays and fibers, respectively. The length of the cells was determined by direct measurement of individual cells, and the misalignment of fibers was determined by measuring the angle with respect to the axial direction. The length of the cells and the misalignment of fibers were measured only in MD balsa, from the axial–tangential plane. The cell wall thickness was determined by direct measurement of individual cell walls, with several measurements taken from the same wall. The cell wall thickness in vessels and rays was only determined in MD balsa. The solid fraction of each type of cell was calculated using the mean lumen dimensions and cell wall thickness, and assuming elliptical, rectangular or hexagonal cells. The volume fraction of vessels and rays was calculated by measuring the area fraction of each in cross section, according to the Delesse principle. The volume fraction of fibers was calculated by subtracting the volume fraction of rays and vessels from the total wood volume.

The thickness of the cell wall layers was measured using transmission electron microscopy. Small LD and HD balsa cubes were embedded in Spurr's resin and placed under vacuum for 48 h to complete impregnation. Thin sections (about 80 nm) were then cut from the embedded cubes with an ultramicrotome (Leica Ultracut UCT) equipped with a diamond knife. The sections were observed in a FEI Tecnai F20 field emission transmission electron microscope (FE-TEM), operated at an accelerating voltage of 120 kV. The TEM was calibrated to within 1 % for all magnifications. Micrographs were taken from sections without staining, and the thickness of the cell wall layers in LD and HD balsa was determined by direct measurement of individual layers, using the software ImageJ 1.45 s.

X-ray scattering

The cellulose MFA, crystallite dimensions and degree of crystallinity in balsa wood samples of various densities were measured by wide-angle X-ray scattering (WAXS) using three different geometries: perpendicular transmission (PT), symmetric transmission (ST) and symmetric reflection (SR). PT measurements were performed with a setup consisting of a Seifert ID 3003 X-ray generator (voltage 36 kV, current 25 mA) equipped with a Cu tube, a collimating Montel multilayer monochromator (Incoatec, wavelength 0.1542 nm), and a MAR345 image plate detector (Marresearch, sample-to-detector distance 12 cm). ST and SR measurements were performed with a four-circle goniometer (422/511, Huber), an X-ray generator (ID 3003, Seifert), a sealed X-ray tube with a Cu anode, a ground and bent Ge monochromator (616-2 Huber, wavelength 0.1541 nm) and a NaI(Tl) scintillation counter. Instrumental broadening was calculated from a silver behenate sample in PT mode (0.35° for $2\theta = 23°$) and from a hexamethylenetetramine $(CH_2)_6N_4$ sample in ST and SR modes (0.27° for $2\theta = 34.7°$). Air scattering background was measured separately for each WAXS geometry. Data corrections and calibration of the scattering angle were conducted according to Penttilä et al. (2013). The crystal structure of cellulose Iβ proposed by Nishiyama et al. (2002) was used as a model for crystalline cellulose.

The MFA distribution was determined from the cellulose Iβ reflection 004 ($2\theta = 34.7°$) in ST mode, in order to minimize the effects of cell shape (Cave 1997; Andersson et al. 2000). Additional peaks observed in the azimuthal profile, arising from weak neighboring reflections, were fitted with Gaussian functions and subtracted from the intensity profile. A Gaussian peak pair was then fitted to the resulting profile to model the reflections from the front and back cell walls. The MFA distribution was obtained from the front cell wall fit.

Cellulose crystallite width was determined from the cellulose Iβ reflection 200 ($2\theta = 23°$) in PT mode, and crystallite length was determined from the cellulose Iβ reflection 004 ($2\theta = 34.7°$) in ST mode. An amorphous contribution to the experimental diffraction pattern was estimated by measuring a sulfate lignin sample (Andersson et al. 2003). Crystallite sizes were calculated from the full width at half maximum (FWHM) using the Scherrer formula (see Andersson et al. 2003; Penttilä et al. 2013).

The relative degree of crystallinity was determined in PT mode by performing a linear least squares fit to 27 cellulose Iβ peak intensities and to the amorphous background. In addition, a texture-corrected degree of crystallinity was calculated, for one balsa sample, as a weighted mean of crystallinities determined with a combination of ST and SR geometries. The weights 2/3 and 1/3 for the ST and SR modes, respectively, were applied (Paakkari et al. 1988: Andersson et al. 2003). The crystalline contribution was modeled by fitting the 15 strongest reflections of cellulose Iβ, with the widths of the major peaks being calculated from a 36-chain crystallite model (Ding and Himmel 2006). Width variation of 10 % and position variation of 0.5° were allowed for the reflection peaks in a nonlinear least squares fit. The intensities of the reflection peaks were essentially free-fitting parameters. The crystallinity values were found by minimizing the R^2 goodness of the fit as a function of the amorphous background multiplying coefficient.

Chemical composition

The chemical composition was determined for LD, MD and HD balsa. First, the extractive content was determined gravimetrically after extraction with acetone for 6 h in a Soxhlet apparatus. Then, the carbohydrates and lignin composition of the extractive-free balsa was determined according to the analytical method NREL/TP-510-42618, issued by the US National Renewable Energy Laboratory (NREL). Briefly, about 300 mg of dry wood was dissolved in 3 ml of 72 % w/w sulfuric acid for 1 h at 30 °C. Subsequently, 84 ml of deionized water was added to bring the sulfuric acid down to 4 % w/w, and the mixture was placed in an autoclave for 1 h at 121 °C (pressure about 2.1 bars). Upon cooling, the acid-insoluble (Klason) lignin was recovered by filtration and determined gravimetrically. The acid-soluble lignin (ASL) in the acidic filtrate was determined in a Shimadzu UV-2550 spectrophotometer at a wavelength of 205 nm. The monosaccharides in the filtrate were determined by high-performance anion-exchange chromatography with pulse amperometric detection in a Dionex ICS-3000 system. Acetyl groups in wood were calculated from the acetic acid content in the filtrate, determined by high-performance liquid chromatography (HPLC) in a Dionex 3000 Ultimate system. The ash content in balsa was determined according to the analytical method NREL/TP-510-42622. All samples were analyzed in duplicate.

Results and discussion

Microstructure of balsa wood

The main cell types identified from the cross section of balsa wood were the vessels, the rays and the fibers (Fig. 1). The vessels typically had an elliptical shape and were elongated in the radial direction (Fig. 2a). The diameter (D) of the vessels was between 220 and 320 μm (Table 1), mostly in agreement with values given by Vural and Ravichandran (2003) and Da Silva and Kyriakides (2007). The vessels were composed of relatively short elements (Fig. 2b), although a considerable

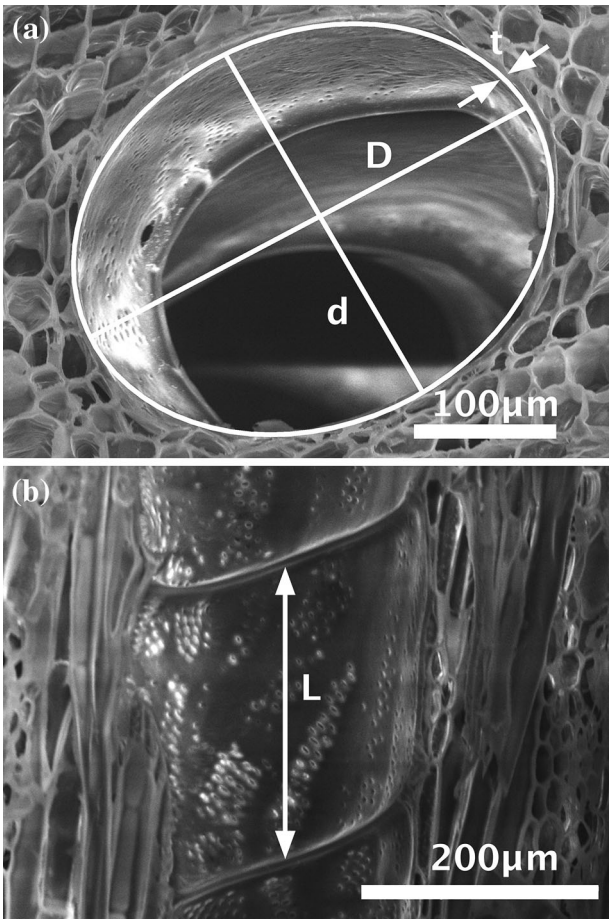

Fig. 2 SEM micrographs of medium-density balsa showing the geometry and cell wall thickness of a vessel element **a** in cross section and **b** in the axial–tangential plane

variability in length existed. Some vessels were found in groups or clusters, arranged radially and with their adjacent walls flattened (Fig. 3). The thickness of the double cell wall (t) between a vessel and another cell type was about 4 µm in MD balsa. The double intervessel walls (T) were considerably thicker, in the order of 9.5 µm. The thickness of the intervessel walls might be a reinforcement mechanism to minimize the risk of implosion in the vessels pipeline by negative water pressures (Hacke et al. 2001). Because vessels are large empty voids within the xylem structure, one might expect their volume fraction to be higher in wood with lower density. However, the volume fraction of vessels increased from LD to HD balsa (Table 1), possibly due to increased fluid transport requirements in HD balsa.

The rays, or radial parenchyma cells, had a rectangular geometry when viewed from the cross section, but a somewhat oval shape when viewed along the axial–

Table 1 Dimensions, volume fraction and solid fraction of main cell types in balsa wood of different densities

	LD balsa	MD balsa	HD balsa
Air-dry density (kg/m^3)	64	163	274
Vessels			
D (μm)	220.4 ± 31.0 (14)	320.8 ± 31.1 (23)	258.8 ± 38.6 (39)
d (μm)	156.6 ± 21.5 (14)	251.0 ± 18.5 (23)	206.6 ± 24.0 (39)
L (μm)	n.d.	382.1 ± 121.1 (19)	n.d.
t (μm)	n.d.	4.0 ± 1.1 (99)	n.d.
T (μm)	n.d.	9.5 ± 1.5 (70)	n.d.
Volume fraction (%)	2.8 ± 0.5 (4)	6.6 ± 1.1 (4)	8.8 ± 2.1 (8)
Solid fraction (%)	6.8	4.5	5.5
Rays			
a (μm)	49.6 ± 8.4 (23)	35.8 ± 6.1 (34)	32.5 ± 3.5 (34)
b (μm)	19.4 ± 3.3 (23)	18.2 ± 3.1 (34)	15.8 ± 1.7 (34)
L (μm)	n.d.	30.7 ± 6.0 (60)	n.d.
t (μm)	n.d.	0.9 ± 0.3 (97)	n.d.
Volume fraction (%)	20.9 ± 2.1 (4)	19.9 ± 0.8 (3)	24.8 ± 1.9 (7)
Solid fraction (%)	6.5	7.4	8.3
Fibers			
h (μm)	21.8 ± 4.5 (57)	18.0 ± 4.8 (105)	9.8 ± 3.0 (270)
t (μm)	0.8 ± 0.2 (50)	1.8 ± 0.5 (125)	2.2 ± 0.8 (250)
L (μm)	n.d.	755.3 ± 122.2 (38)	n.d.
θ (°)	n.d.	6.1 ± 2.0 (30)	n.d.
Volume fraction (%)	76.3	73.5	66.4
Solid fraction (%)	4.3	10.8	21.5

Symbols defined in Figs. 2, 3, 4 and 5

Mean values ± standard deviation, with number of measurements in parentheses

n.d. not determined

tangential plane (Fig. 4). The rays in balsa wood were multiseriate, often comprising 4–6 cells in width and tens of cells in height. The rays in LD balsa appeared to be slightly larger than in MD and HD balsa (Table 1). The thickness of the double cell wall between rays in MD balsa was only about 0.9 μm. Despite the thin cell wall, rays may have a substantial influence on the radial tensile strength of wood (Burgert and Eckstein 2001). The volume fraction of rays was similar in LD and MD balsa, but somewhat larger in HD balsa (Table 1).

The fibers in balsa wood had an irregular polygonal shape in cross section, often resembling a hexagon; for simplicity, they were modeled as regular hexagons (Fig. 5). As indicated by the length of the cell side (*h*) in Table 1, the fiber size was found to decrease with increasing balsa density. The diameter of the cell lumen, based on values of h, varied roughly between 20 and 45 μm, while the fiber length measured in MD balsa was about 755 μm. Similar fiber dimensions have been

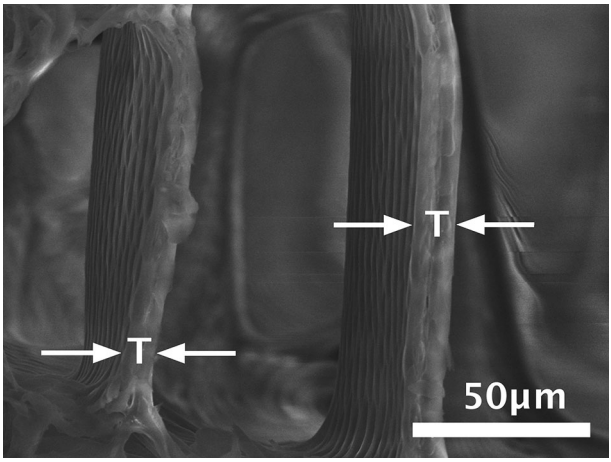

Fig. 3 SEM micrograph of the cross section of medium-density balsa showing thick and flattened walls between adjacent vessels

previously reported for balsa (Easterling et al. 1982; Da Silva and Kyriakides 2007) and for hardwoods in general (Fengel and Wegener 2003). The thickness of the double cell wall increased nearly threefold from LD to HD balsa, from about 0.8 up to 2.2 µm (Table 1). The volume fraction of fibers was calculated by subtracting the volume fraction of rays and vessels from the total wood volume. Accordingly, the volume fraction of fibers decreased with increasing wood density, with fibers accounting for between two-thirds and slightly over three quarters of the balsa wood volume, less than the 80–90 % reported by Easterling et al. (1982) and Da Silva and Kyriakides (2007).

Fibers in the xylem were aligned axially along the trunk of the tree. However, some fibers showed a change in orientation in the axial–tangential plane, particularly where rays penetrated the wood structure (Fig. 5b). The mean fiber misalignment (θ) in MD balsa was 6.1° (Table 1), similar to the values reported by Da Silva and Kyriakides (2007) and somewhat lower than the 9° reported by Vural and Ravichandran (2003). From a mechanical point of view, fiber misalignment is important because it leads to the development of shear stresses during compression and to initiation of failure by kinking in high-density balsa (Vural and Ravichandran 2003; Da Silva and Kyriakides 2007). In Fig. 5b, one can also observe some brick-like cells located near the ray pockets. These cells are longitudinal parenchyma, and although they were clearly visible in the axial–tangential plane, they were difficult to identify from the cross section. Therefore, the ray volume fraction determined in this study may include to some extent a fraction of longitudinal parenchyma cells.

The cell dimensions and cell wall thicknesses in Table 1 were used to calculate the solid fraction of fibers, vessels and rays, having hexagonal, elliptical and rectangular geometries, respectively. The fiber solid fraction was also determined by analyzing selected SEM micrographs, and the results (not shown) were found to be comparable to those obtained by using mean fiber dimensions and cell wall thickness. The solid fraction of the fibers increased about fivefold from LD to HD balsa, which is a

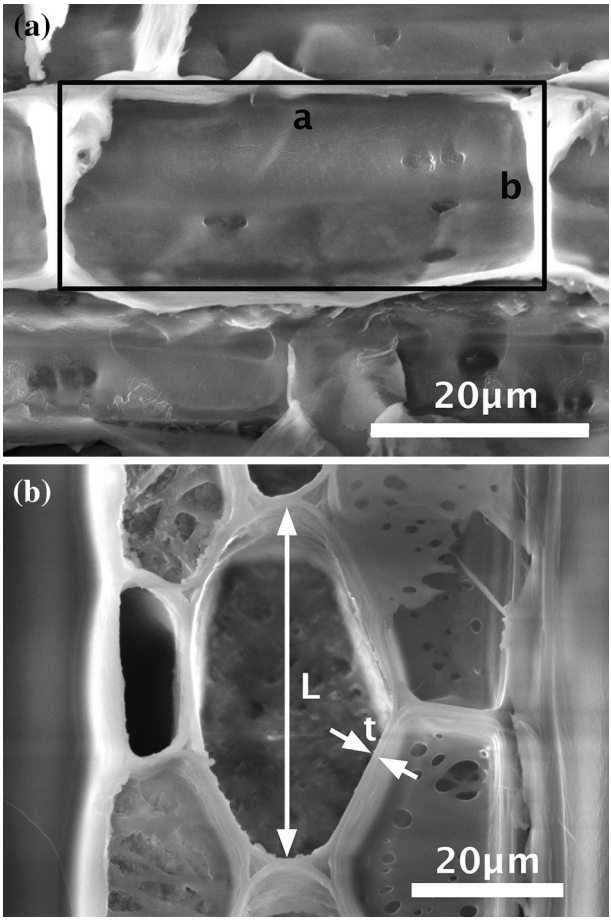

Fig. 4 SEM micrographs of medium-density balsa showing the geometry and cell wall thickness of ray cells **a** in cross section and **b** in the axial–tangential plane

consequence of balsa fibers having smaller lumina and thicker cell walls with increasing wood density. This is similar to hardwoods of temperate zones, in which high-density latewood fibers are smaller and have thicker cell walls than low-density earlywood fibers (Fengel and Wegener 2003). The solid fraction of vessels and rays only showed a small variation with density (Table 1). It should be noted, however, that the solid fractions of vessels and rays in LD and HD balsa are approximate, because they were determined by using the cell wall thicknesses of MD balsa.

Based on the volume and solid fractions listed in Table 1, and noting that the moisture content of the wood was 5–7 %, the dry density of LD, MD and HD balsa, ρ_{balsa}, was approximated as follows:

$$\rho_{\text{balsa}} = \rho_{\text{s}}(V_{\text{f}}S_{\text{f}} + V_{\text{v}}S_{\text{v}} + V_{\text{r}}S_{\text{r}}) \quad (1)$$

where ρ_{s} is the dry cell wall density (1,469 kg/m^3, Kellogg and Wangaard 1969), V_{f}, V_{v} and V_{r} are the volume fractions and S_{f}, S_{v} and S_{r} are the solid fractions of fibers,

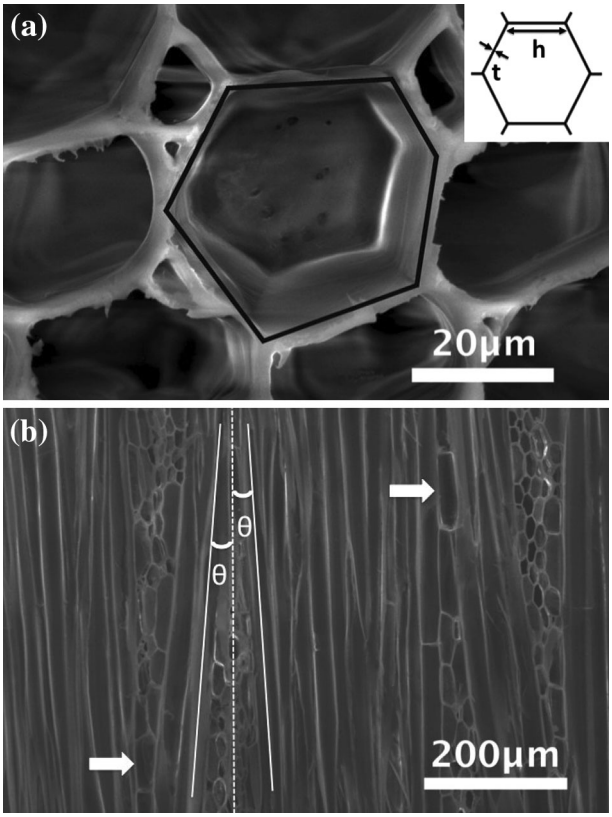

Fig. 5 SEM micrographs of medium-density balsa showing **a** the geometry of fibers in cross section and (*inset*) their approximation as regular hexagons and **b** the misalignment of fibers in the axial–tangential plane and longitudinal parenchyma cells (indicated by *arrows*)

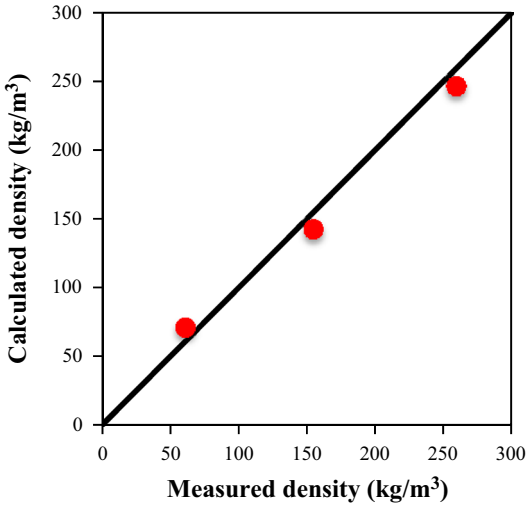

Fig. 6 Calculated balsa density plotted against measured density. Calculated density is the sum of the density of vessels, rays and fibers (see Eq. 1)

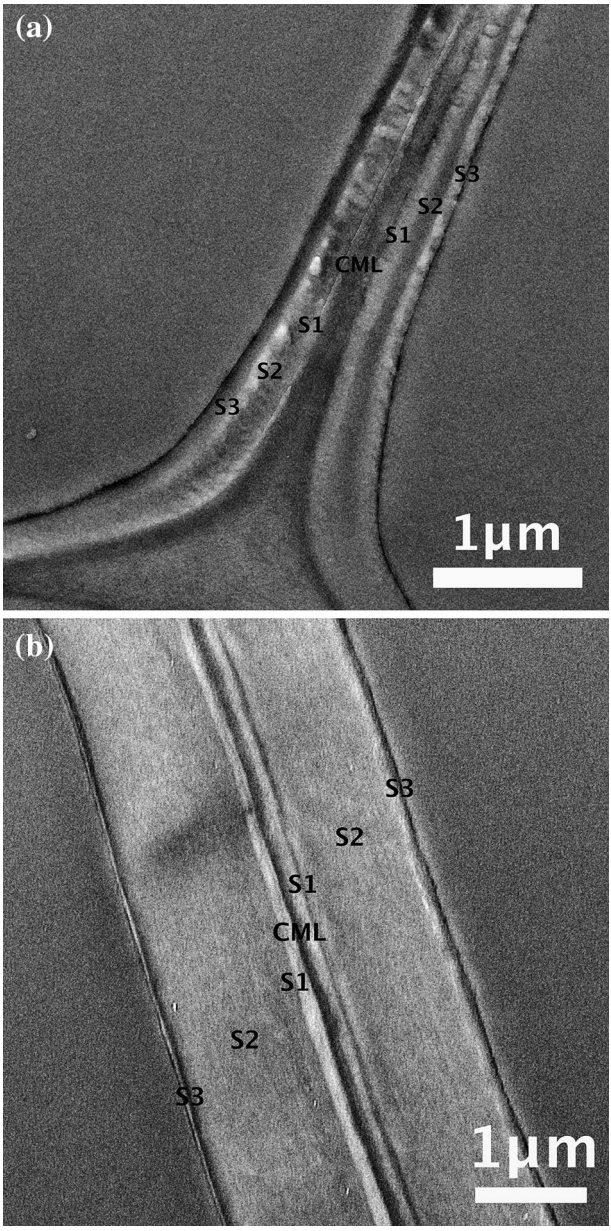

Fig. 7 TEM micrographs showing the different cell wall layers in **a** low-density balsa and **b** high-density balsa

vessels and rays, respectively. The good agreement between measured and calculated balsa densities, shown in Fig. 6, supports the validity of the cell dimensions and volume and solid fractions determined in this study.

Table 2 Thickness of cell wall layers in fibers of balsa wood of different densities

	LD balsa	HD balsa
Air-dry density (kg/m^3)	75	264
Thickness (μm)		
CML/2	0.08 ± 0.02 (78)	0.13 ± 0.06 (119)
S1	0.11 ± 0.04 (69)	0.16 ± 0.06 (116)
S2	0.12 ± 0.04 (66)	1.09 ± 0.38 (113)
S3	0.10 ± 0.06 (68)	0.12 ± 0.03 (114)
Total (*t*/2)	0.41	1.49

Mean values ± standard deviation, with number of measurements in parentheses

Ultrastructure of the fiber cell wall

The cell wall layers in LD and HD balsa fibers are shown in Fig. 7. The different cell wall layers could be easily identified by TEM without need for staining with potassium permanganate ($KMnO_4$). It is clear that the increase in fiber cell wall thickness with increasing balsa density was predominantly due to the presence of a thicker S2 layer, with only a small contribution from the compound middle lamella (CML), S1 and S3 layers (Table 2). In LD balsa, the S2 layer was as thick as the S1 and S3 and accounted for about 30 % of the cell wall thickness. In HD balsa, the S2 was 7–9 times thicker than the S1 and S3 and accounted for about 73 % of the cell wall thickness (Table 2). For LD balsa, the mean cell wall thickness (*t*/2) from Table 2 was comparable to that from Table 1. For HD balsa, it was somewhat higher, although still within the variability limits indicated by the standard deviation.

The S2 is considered the most important layer in the cell wall with respect to axial mechanical properties of wood, and particularly with respect to stiffness (Cave 1968). This is due to the greater thickness of the S2 layer, but also to its lower MFA (Barnett and Bonham 2004; Donaldson 2008). In this study, the MFA distribution in the S2 layer of balsa wood was investigated by X-ray diffraction. In Fig. 8, the experimental and fitted model for the angular intensity profile of the reflection 004 in ST mode, as well as the resulting MFA distribution, is shown for a selected MD balsa sample (159 kg/m^3). The intensity profile and the MFA distribution were similar for a wide range of balsa densities (curves not shown), which seems to support previous observations that wood density and MFA do not correlate, despite low-density earlywood fibers generally showing higher MFAs than latewood fibers (Evans et al. 2000; Fang et al. 2006; Donaldson 2008). The azimuthal intensity profiles measured at the scattering angle 34.7° showed a clear peak from the reflection 004, but other well-separated and symmetric peak pairs of lower intensity were also visible at large azimuthal angles (data not shown). The latter were fitted with Gaussian functions and subtracted from the intensity profile in order to produce pure reflection 004 data (Fig. 8a). Similar peaks were not visible in the azimuthal intensity profile of the reflection 200 (scattering angle 22.6°; data not shown), which confirmed that their presence in the intensity profile of the reflection 004 originated from neighboring reflections, presumably the reflections 203 and $\bar{1}23$ at the azimuthal angle ±40° and the reflections $\bar{1}31$ and

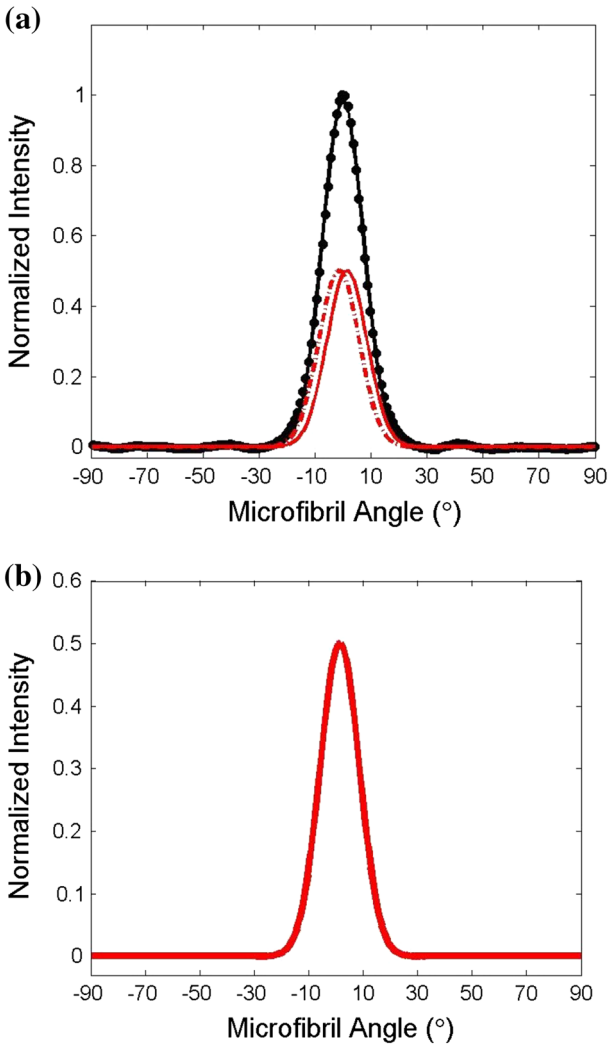

Fig. 8 **a** Normalized experimental and fitted model for angular intensity profile of the reflection *004* in symmetric transmission geometry for a medium-density balsa sample. *Black circles* experimental intensity profile; *black line* fitted model; *lighter lines* individual Gaussian functions for front (*solid line*) and back (*dashed line*) cell walls. **b** Microfibril angle distribution obtained from the front cell wall fit in **a**

301 at the angle ±75° (Andersson et al. 2000). The Gaussian curve for the front cell wall fit, representing the MFA distribution, showed a narrow distribution with a maximum centered at low angles (Fig. 8b). The calculated mean MFA for all balsa densities was 1.4°, and the mean standard deviation for the MFA was 7.4° (Table 3). These values are lower than those reported for birch (Bonham and Barnett 2001) and poplar (Fang et al. 2006), but similar to those determined for oak and beech (Lichtenegger et al. 1999).

Table 3 Cellulose crystallite dimensions, degree of crystallinity and mean MFA in balsa wood of different densities

Air-dry density (kg/m^3)	Mean MFA (±3°)	Standard deviation of MFA (±3°)	Degree of crystallinity (±3 %)	Crystallite width (±0.2 nm)	Crystallite length (±1 nm)
86	1.6	7.8	38.5	3.0	22.6
128	1.1	7.1	37.6	3.1	28.3
145	1.4	7.0	38.3	3.1	29.9
159	1.4	7.1	39.0	3.1	24.3
180	1.4	7.6	38.9	3.1	28.2
211	1.5	7.7	40.4	3.0	29.6
Average	1.4	7.4	38.8	3.1	27.2

Table 4 Chemical composition of balsa wood of different densities

	LD balsa	MD balsa	HD balsa
Air-dry density (kg/m^3)	86	167	284
Chemical composition (wt%)			
Glucose[a]	40.1	41.5	45.3
Mannose[a]	1.6	2.3	3.3
Arabinose[a]	0.3	0.2	0.1
Rhamnose[a]	1.1	0.7	0.5
Galactose[a]	0.9	0.5	0.3
Xylose[a]	14.4	16.3	15.4
Acetyl groups	5.7	5.3	5.2
Klason lignin	20.5	22.2	23.3
Acid-soluble lignin	3.4	2.7	2.6
Extractives[b]	2.9	2.0	1.0
Ash	1.8	1.0	0.3
Total	92.7	94.7	97.3

[a] Determined as anhydrosugars

[b] Determined after extraction with acetone

Cellulose microfibrils contain both amorphous and highly ordered crystalline regions. The relative degree of crystallinity in balsa, determined from the reflection 200 in PT mode, was found to be about 39 %, irrespective of density (Table 3). The relative degree of crystallinity in a wood sample may depend on the orientation of the scattering planes (texture effects, such as the MFA distribution) and the choice of measurement geometry (Paakkari et al. 1988; Andersson et al. 2003). In order to reduce texture effects on the determination of crystallinity, two symmetric geometries were combined with appropriate weights to determine a texture-corrected degree of crystallinity of a selected MD balsa sample (159 kg/m^3). The relative degree of crystallinity determined in ST and SR modes was 31.3 and 45.8 %, respectively. Applying the corresponding 2/3 and 1/3 weights, the texture-corrected crystallinity value was 36.2 % (±5 %), not far from the 39.0 % determined in PT mode (Table 3). Considering that the cellulose content in balsa

was between 40 and 45 %, then cellulose crystallinity was about 80–90 %, significantly higher than the 40–60 % determined for other hardwoods such as birch, aspen and oak (Wikberg and Maunu 2004; Penttilä et al. 2013). Similar to the degree of crystallinity, the width of cellulose crystallites was about the same for all balsa densities investigated, while slightly more variation was observed in crystal length (Table 3). The values for crystal width (about 3 nm) and length (20–30 nm) in balsa are in agreement with cellulose crystal dimensions determined for many woods (Hori et al. 2002; Andersson et al. 2003; Peura et al. 2008; Penttilä et al. 2013).

Chemical composition

The measured chemical composition of LD, MD and HD balsa is shown in Table 4. The weight fraction of cellulose, largely represented by the glucose content, was about 40–45 % of the dry wood mass, increasing slightly with density. However, some glucose corresponded to glucomannan, with a glucose–mannose ratio of 1:1–2 in hardwoods (Timell 1967). As the mannose content increased with density, so did the glucose fraction corresponding to glucomannan, and therefore, the difference in cellulose content between balsa densities should be considered minor. The glucomannan content was mostly between 2 and 5 %, while the xylan (xylose and acetyl groups) content was about 21 % of the dry wood mass. The amount of xylose was nearly three times that of acetyl groups, but given their molar masses (132 g/mol for anhydroxylose and 43 g/mol for acetyl) the xylose–acetyl ratio was about 1:1, which is higher than the 1:0.7 usually reported for hardwoods (Timell 1967). The lignin (Klason and ASL) content was around 25 % of the dry wood mass for all densities.

In addition to the cell wall structural components, woods contain a number of different extraneous compounds that are grouped into organic (extractives) and inorganic (ash) matter. The extractive content in balsa was between 1 and 3 %, and the ash content was below 2 % (Table 4). The extractive content is rather low, considering that in tropical woods it often exceeds 5 % of the dry mass (Fengel and Wegener 2003). In this study, only those extractives soluble in organic solvent (acetone) were removed, and thus, additional extractives might be removed by hot water extraction. Both the extractives and the ash content appeared to decrease with increasing balsa density.

The detailed characterization of the composition and structure of balsa wood presented in this study should be useful in developing multi-scale models of the mechanical behavior of balsa, from atomistic simulations of the interactions of the constituents, to coarse-grained models of cellulose microfibrils in the matrix of hemicelluloses and lignin, to detailed finite element cellular solids models.

Conclusion

Fibers were the main contributor to large density variations found in balsa wood. The volume fraction of fibers decreased slightly with increasing balsa density, but

their solid fraction increased at least fivefold, owing to smaller cell lumina and thicker cell walls. The increase in cell wall thickness was predominantly due to a thicker S2 layer. Cellulose microfibrils in the S2 were highly aligned with the fiber axis, with a mean MFA in the vicinity of 1.4°. The cellulose crystallites in the microfibrils were about 3 nm in width and 20–30 nm in length. The degree of cellulose crystallinity was between 80 and 90 %, significantly higher than previously reported for other woods. The low MFA, coupled with the high crystallinity, is expected to confer excellent axial mechanical properties to balsa wood.

Acknowledgments Funding provided by BASF through the North American Center for Research on Advanced Materials (Program Manager Dr. Marc Schroeder; Dr. Holger Ruckdaeschel and Dr. Rene Arbter) is gratefully acknowledged. Mr. Timo Ylönen and Ms. Rita Hatakka from Aalto University (Finland) are thanked for their support in determining the chemical composition of balsa wood. Dr. Paavo Penttilä and Dr. Seppo Andersson from University of Helsinki (Finland) are thanked for their support with the X-ray scattering measurements and data analysis. Carolyn Marks is thanked for her work on sample preparation and TEM imaging, performed at the Center for Nanoscale Systems (CNS), a member of the National Nanotechnology Infrastructure Network (NNIN), which is supported by the National Science Foundation under NSF Award No. ECS-0335765. CNS is part of Harvard University.

References

Andersson S, Serimaa R, Tokkeli M, Paakkari T, Saranpää P, Pesonen E (2000) Microfibril angle of Norway spruce (*Picea abies* (L.) Karst.) compression wood: comparison of measuring techniques. J Wood Sci 46:343–349

Andersson S, Serimaa R, Paakkari T, Saranpää P, Pesonen E (2003) Crystallinity of wood and the size of cellulose crystallites in Norway spruce (*Picea abies*). J Wood Sci 49:531–537

Andersson S, Wikberg H, Pesonen E, Maunu SL, Serimaa R (2004) Studies of crystallinity of Scots pine and Norway spruce cellulose. Trees-Struct Funct 18:346–353

Barnett JR, Bonham VA (2004) Cellulose microfibril angle in the cell wall of wood fibres. Biol Rev 79:461–472

Bergander A, Salmén L (2002) Cell wall properties and their effects on the mechanical properties of fibers. J Mater Sci 37:151–156

Bonham VA, Barnett JR (2001) Fibre length and microfibril angle in Silver birch (*Betula pendula* Roth). Holzforschung 55:159–162

Burgert I, Eckstein D (2001) The tensile strength of isolated wood rays of beech (*Fagus sylvatica* L.) and its significance for the biomechanics of living trees. Trees-Struct Funct 15:168–170

Cave ID (1968) The anisotropic elasticity of the plant cell wall. Wood Sci Technol 2:268–278

Cave ID (1997) Theory of X-ray measurement of microfibril angle in wood. Part 2: the diffraction diagram. X-ray diffraction by materials with fibre type symmetry. Wood Sci Technol 31:225–234

Da Silva A, Kyriakides S (2007) Compressive response and failure of balsa wood. Int J Solids Struct 44:8685–8717

Ding SY, Himmel ME (2006) The maize primary cell wall microfibril: a new model derived from direct visualization. J Agric Food Chem 54:597–606

Donaldson L (2008) Microfibril angle: measurement, variation and relationships—a review. IAWA J 29:345–386

Easterling KE, Harrysson R, Gibson LJ, Ashby MF (1982) On the mechanics of balsa and other woods. P R Soc Lond A 383:31–41

Evans R, Stringer S, Kibblewhite RP (2000) Variation of microfibril angle, density and fibre orientation in twenty-nine Eucalyptus nitens trees. Appita 53:450–457

Fang S, Yang W, Tian Y (2006) Clonal and within-tree variation in microfibril angle in poplar clones. New For 31:373–383

Fengel D, Stoll M (1973) On the variation of the cell cross area, the thickness of the cell wall and of the wall layers of sprucewood tracheids within an annual ring. Holzforschung 27:1–7

Fengel D, Wegener G (2003) Wood—chemistry, ultrastructure, reactions. Verlag Kessel, Remagen
Fernandes AN, Thomas LH, Altaner CM, Callow P, Forsyth VT, Apperley DC, Kennedy CJ, Jarvis MC (2011) Nanostructure of cellulose microfibrils in spruce wood. P Natl Acad Sci USA 108:E1195–E1203
Fletcher MI (1951) Balsa—production and utilization. Econ Bot 5:107–125
Hacke UG, Sperry JS, Pockman WT, Davis SD, McCulloh KA (2001) Trends in wood density and structure are linked to prevention of xylem implosion by negative pressure. Oecologia 126:457–461
Hori R, Müller M, Watanabe U, Lichtenegger HC, Fratzl P, Sugiyama J (2002) The importance of seasonal differences in the cellulose microfibril angle in softwoods in determining acoustic properties. J Mater Sci 37:4279–4284
Kellogg RM, Wangaard FF (1969) Variation in the cell wall density of wood. Wood Fiber Sci 1:180–204
Lichtenegger H, Reiterer A, Stanzl-Tschegg SE, Fratzl P (1999) Variation of cellulose microfibril angles in softwoods and hardwoods—a possible strategy of mechanical optimization. J Struct Biol 128:257–269
Nishiyama Y, Langan P, Chanzy H (2002) Crystal structure and hydrogen-bonding system in cellulose Iβ from synchrotron X-ray and neutron fiber diffraction. J Am Chem Soc 124:9074–9082
Paakkari T, Blomberg M, Serimaa R, Järvinen M (1988) A texture correction for quantitative X-ray powder diffraction analysis of cellulose. J Appl Crystallogr 21:393–397
Penttilä PA, Kilpeläinen P, Tolonen L, Suuronen JP, Sixta H, Willför S, Serimaa R (2013) Effects of pressurized hot water extraction on the nanoscale structure of birch sawdust. Cellulose 20:2335–2347
Peura M, Müller M, Vainio U, Sarén MP, Saranpää P, Serimaa R (2008) X-ray microdiffraction reveals the orientation of cellulose microfibrils and the size of cellulose crystallites in single Norway spruce tracheids. Trees-Struct Funct 22:49–61
Solden PD, McLeish RD (1976) Variables affecting the strength of balsa wood. J Strain Anal 11:225–234
Timell TE (1967) Recent progress in the chemistry of wood hemicelluloses. Wood Sci Technol 1:45–70
Vural M, Ravichandran G (2003) Microstructural aspects and modeling of failure in naturally occurring porous composites. Mech Mater 35:523–536
Wikberg H, Maunu SL (2004) Characterisation of thermally modified hard- and softwoods by ^{13}C CPMAS NMR. Carbohydr Polym 58:461–466